Hindawi
Advances in Condensed Matter Physics
Volume 2018, Article ID 4950787, 6 pages
https://doi.org/10.1155/2018/4950787

*Research Article*

# Micro/Nanofiber with Hollow Silica Nanoparticles Thin-Film for Airborne Molecular Contaminants Real-Time Sensing

**Longfei Niu,[1] Guorui Zhou,[1] Xinxiang Miao,[1] Xiaodong Yuan,[1] Rahul Kumar,[2] Hao Liu,[1] Yilan Jiang,[1] Xinshu Zou,[1] Hai Zhou,[1] and Haibing Lü[1]**

[1]*Laser Fusion Research Center, China Academy of Engineering Physics, Mianyang 621900, China*
[2]*Faculty of Engineering & Environments, Northumbria University, Newcastle Upon Tyne NE1 8ST, UK*

Correspondence should be addressed to Haibing Lü; haibinglv@163.com

Received 15 March 2018; Revised 14 May 2018; Accepted 17 May 2018; Published 11 June 2018

Academic Editor: Jiaqi Wang



A novel chemical sensing approach detecting airborne molecular contaminants (AMCs) or compounds is demonstrated by using single-mode optical microfibre (OMF) coated with hollow silica nanoparticles (HSNs). The concentration of AMCs, which were volatilized on the surface of the tapered microfibre coated with HSNs, influences the transmission loss of the microfibre. Tapered OMF was fabricated using a high-precision electrically controlled setup, and coatings of HSNs were prepared by meniscus coating method. The transmission loss of three OMFs with different diameters and the same thick coating were tested to determine the relationship between AMC concentrations and transmission loss of coated OMFs. Experimental results showed that the transmission loss increases with increasing concentration of AMCs. The sensitivity for volatile simethicone was 0.0263 dB/mg/m$^3$ obtained by the coated OMF with diameter of 2.5 $\mu$m, and the sensitivity values of coated OMF with diameters of 5 $\mu$m and 6 $\mu$m were 0.0024 and 0.0018 dB/mg/m$^3$, respectively. Thus the proposed coated OMF can be used in enclosed space for AMCs sensing.

## 1. Introduction

In the past decades, important applications for optical fibre sensors have been developed in various fields, such as in sensing temperature, magnetic field, strain, and pressure, and they can work at different conditions based on various structures or disparate optical transmission mechanisms [1–5]. However, normal single-mode optical fibres cannot directly satisfy the particular demands of chemical sensing, but the microfibre has the potential to be used in chemical sensing [6, 7], especially with the development of the functionalization of microfibres. The coated microfibre forms a three-layered waveguide. A dielectric microfibre core is bounded by the coating and the surrounding air. Generally, if the coating is contaminated, the refractive index (RI) of the intermediate cladding will change and affect the evanescent field of light propagating along the microfibre, and consequently the transmission loss of the microfibre will be changed with the RI changing of the surrounding medium [8]. Thus, it is promising to design microfibre sensors with higher sensitivity and reliability.

For the coated microfibres, the coated layer plays an important role in the sensitivity of chemical sensing. Luo et al. [9] proposed a microfibre sensor with a cluster layer consisting of silver nanoparticles to probe concentrations of melamine and reported that the sensitivity can reach 1ug/mL. Jesus et al. [10] fabricated a fibre-optic sensor coated with porous silica xerogel film for the detection of airborne molecular contaminants, and the experimental results showed that there was a stronger interaction between methanol and ethanol with the silanol groups on the film, but the adsorption process was irreversible. Park et al. [11] proposed a selective chemical sensing approach by using a poly(dimethyl siloxane)-coated fibre Bragg grating for detecting various volatile organic compounds. Liu et al. [12] reported a high sensitivity ammonia sensor based on a tapered small core single-mode fibre structure for the measurement of ammonia concentration in water, and they estimated that the resolution

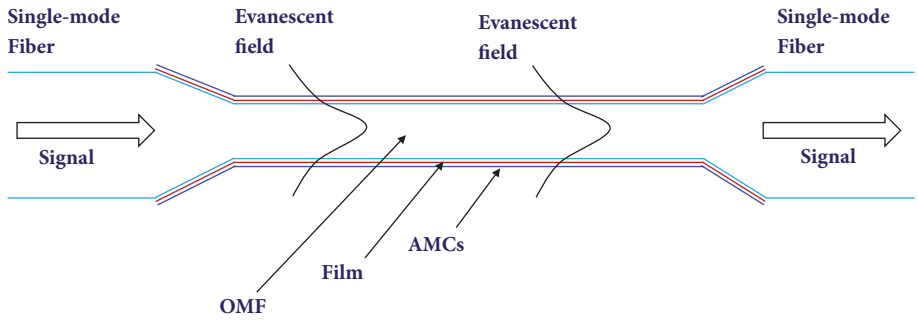


Figure 1: Principle of molecular contaminants adhered on microfibre with HSNs film.

for ammonia concentration in water can reach 4 ppb. Besides, silica nanoparticle has been also used for gas or humidity sensing [13, 14]; especially it showed a lower contact angle about 27° in recent approach [15] that means some contamination may easily be adsorbed.

In this paper, we proposed an OMF sensor coated with HSNs for the detection of AMCs. OMFs with different diameters were fabricated using a high-precision electrically controlled setup, which was consisting of a microheater, three motorized precision translation stages, and a main control box. The shape-controlled HSNs were synthesized by a soft-templating method which includes changing the contents of the template, poly(acrylic acid) (PAA) [16], and the HSNs were coated on the surface of the microfibre uniformly by the meniscus coating method. The sensitivity of coated microfibres with different diameters was measured, and the relationship between the concentrations of AMC and the transmission loss of microfibre was determined. The proposed sensor has the advantages of competitive durability and fast and real-time detection based on the evanescent field coupling between the OMF and the polymer planar waveguide.

## 2. Sensing Mechanism

The sensing mechanism of coated microfibre is based on the change of transmission loss due to the RI changing of the coatings caused by the adsorption of AMCs (simethicone) on the HSNs film. When the sensitive waist region of the OMF with HSN film is contaminated by the AMCs, the RI of the coating will be changed and can be calculated by the following equation:

$$n_p = \sqrt{\sum_m n_m^2 \nu_{\partial m}} \quad (1)$$

where $n_p$ and $n_m$ represent the equivalent RI of the coating and the RI of the HSN film or the AMCs, respectively, $m$ represents the different chemical categories, and $\nu_{\partial m}$ is the volume fraction of $m$ layer.

With the increase of the deposition of AMCs on the HSNs, the energy of evanescent field of OMF is absorbed by the newly formed AMC layer. Thus, the additional transmission loss will increase. The transmission loss of OMF is related to the amount of deposited contaminants, and the mass of contaminants can be obtained according to [17]. The principle of the adhesion of molecular contaminants on OMF with HSN film is shown in Figure 1.

## 3. Experimental Preparation

*3.1. Fabrication of OMF.* The single-mode optical fibre (SMF-28, 9/125 $\mu$m, core/cladding diameter, Corning, Inc.) was tapered by using the conventional heating and drawing method, as shown in Figure 2 (inset). Before tapering, the protective polymer cladding was stripped by the commercial cutting pliers for a length about 60 mm, and then the stripped single-mode optical fibre was clamped on the two translation stages by fibre holders. The optical fibre was heated up to 1600°C by precisely controlling the current of a microheater by a DC power supply (TSX3510P, TTi, Inc.). The movements of the two translation stages were precisely controlled by a programmed controller (TMC-USB Motion Controller, Zolix, Inc.) to draw the fibre to the required diameter with a desired waist length. The fabricated microfibre was then coated with HSNs.

*3.2. Synthesis of HSNs and Meniscus Coating.* The HSNs were prepared by the modified Stöber method [18]. In accordance with previous work [16, 19, 20], 0.15 g PAA was dissolved in 7 mL ammonia hydroxide at room temperature and then mixed with 180 mL of ethanol in a 250-mL glass conical flask. After that, 1 mL Tetraethoxysilicate (TEOS, < 98 %) was gradually injected into the solution within 5 hrs under vigorous magnetic stirring at 30°C. Finally, the synthetic HSN solution (RI 1.2, particle diameter ~40nm) was obtained.

About 0.1 mL of synthetic solution of HSNs was fed into a needle tube, which was placed on the clamp of the translation stage. Then, the translation stage was driven by the programmed motion controller step by step, and the OMF traversed the centre of the liquid drop of the HSN solution. Different thicknesses of HSN coating were obtained by changing the cycle steps of the translation stage. Finally, the pigtail of the OMF coated with HSNs was fusion-spliced to standard FC pigtails so that it can be connected to other optical devices.

*3.3. OMF Sensor System.* Figure 2 showed the schematic diagram of experimental setup of OMF sensor, which is comprised of an optical transmission measurement setup

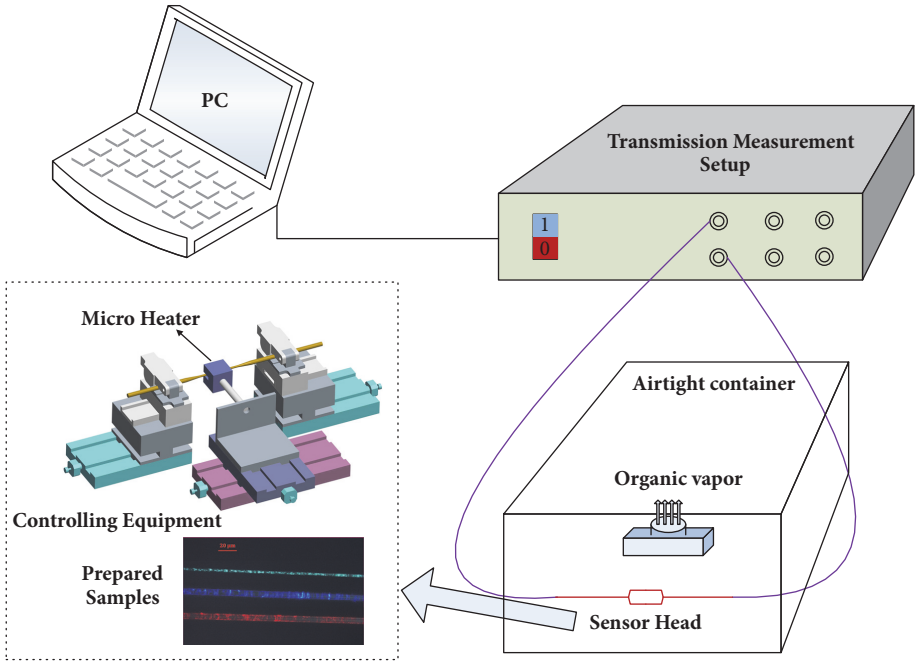


Figure 2: Experimental setup of coated OMF sensor.

(TMS), an airtight chamber, and an electric heater. The AMCs used in the experiment were prepared by heating a beaker filled with simethicone. An input laser beam emitted by a laser diode (RIO, 1mW, $\lambda$ = 1550 nm) from the TMS passed through the coated OMF sensor and entered the terminal of the TMS to measure the transmission loss. In our experiment, the sensor's sensitivity S is defined as $S=\Delta\varphi/C$, where $\Delta\varphi$ represents the additional loss change under different AMC concentrations and C is the AMC concentration, and the additional loss can be calculated by the formula $\Delta\varphi=10\log[P_{out}/P_{in}]$, where $P_{in}$ and $P_{out}$ are the input and output energy, respectively.

## 4. Results and Discussion

*4.1. Influence of HSN Coating on OMF.* The sensitivity of the OMF sensor was monitored during drawing and coating processes. Figure 3 showed the transmission loss of the OMF sensor for different processes. Initially, the transmission loss of the fibre kept a steady state at approximately zero. During the drawing process, the transmission loss decreased with the fibre thinning and reached a constant value of 2.5%. During the coating process, the naked OMF was soaked and the HSNs were absorbed onto the surface of the tapered OMF, and the transmission loss undulated regularly at the first six coating processes. However, with the increase of the coating thicknesses of the OMFs, the transmission loss decreased sharply in the next four coating processes. Finally, the transmission loss reached almost 77%.

The surface morphology of the OMF coated with HSNs was characterized by using a scanning electron microscope (SEM), as shown in Figure 4. The HSN coating layer was not smooth. Due to the existence of the raised portions of

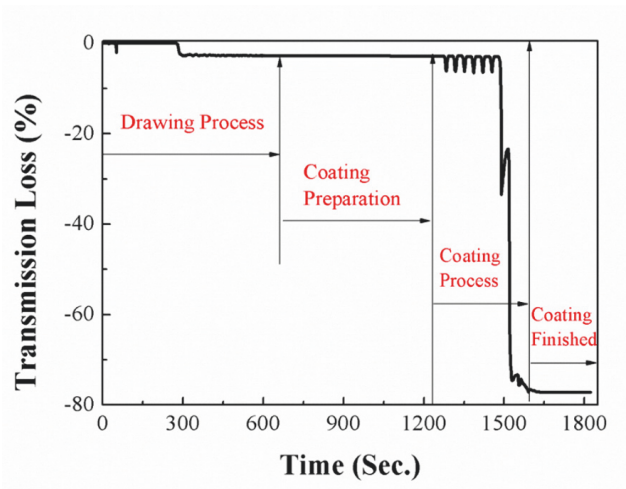


Figure 3: Transmission loss of OFM during drawing and coating processes.

HSN coating, the interface between the AMCs and the HSNs was increased, leading to the increased adsorption of the AMCs onto the HSN layer. Figure 4(b) showed the detailed surface morphology of the HSN coating. The rough surface is comprised of sphere clusters of HSNs. Generally, the HSN coatings acted as the main sensing part of the OMF.

The fabricated OMF sensor was placed on a glass disc located in the container. At the beginning, the original additional loss was tested for five minutes with the purpose of obtaining initial records. Then a beaker filled with simethicone was heated using a controllable heater for ten minutes in order to produce the volatile vapour. The container must be

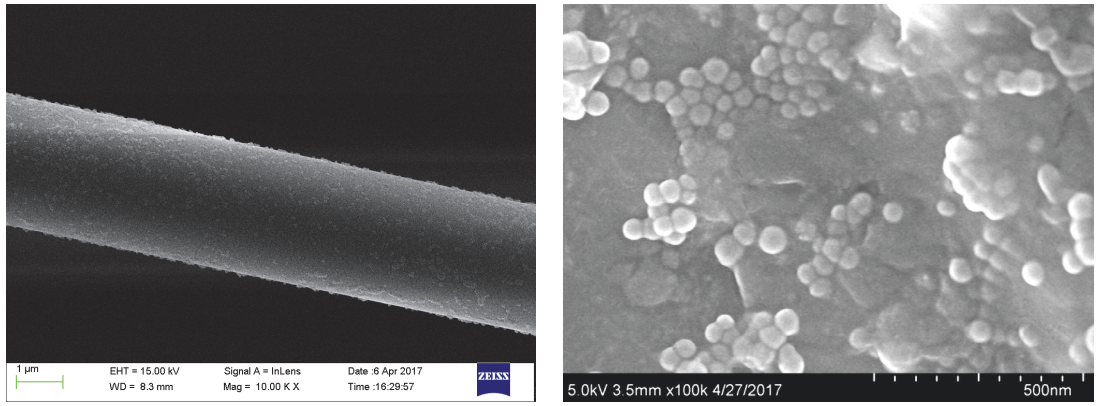


(a) (b)

Figure 4: Surface morphology of the OMF with HSNs (a) at 15kv and 10k × and (b) at 5kv and 100k ×.

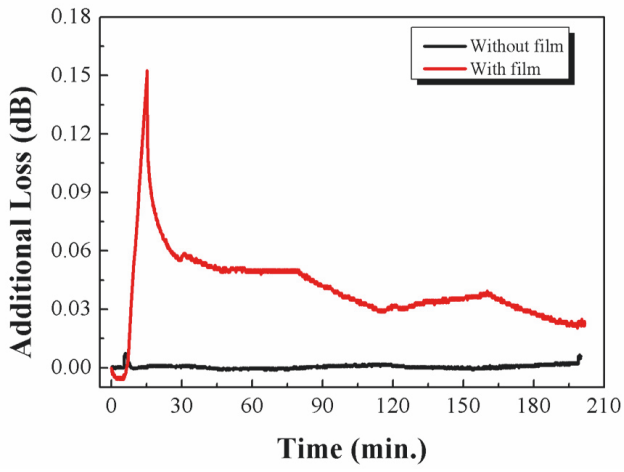


Figure 5: Sensitivity and recovery responses of coated and naked OMF sensors (diameter, ~5 $\mu$m) to AMCs at a concentration of 106.3 mg/m$^3$.

closed so that the prepared OMF with HSNs coating interacts with the AMCs vapour sufficiently during this time. Then the container was opened and the additional loss was observed in real time. As shown in Figure 5, the additional losses of the OMF with and without HSN coating were obtained to assess the sensitivity and recovery of the coated OMF to AMCs with a specific concentration of 106.3 mg/m$^3$. Obviously, the OMF with HSN coating has a highly sensitive response to AMCs when compared with the naked OMF under the same conditions. Thus, the effect of temperature could be ignored because the naked OMF had a lower response to a concentration of 106.3 mg/m$^3$ at 60°C. According to the experimental results, the additional losses for the OMF with HSN coating increased sharply during the initial ten minutes and then decreased gradually with time increasing. Meanwhile, the AMCs were adsorbed and desorbed by the HSNs coating during this process.

*4.2. Measurements of Coated OMF with Different Concentrations of the AMCs and Fibre Diameters.* Figure 6 showed the behavior of the coated OMF sensor at different concentrations of AMCs between 25.7 and 134.2 mg/m$^3$ with three different diameters of 2.5 $\mu$m, 5 $\mu$m, and 6 $\mu$m. It can be seen that, as the concentration increases, the peak of additional loss also increases nonlinearly. This is because the energy of evanescent field around the OMF sensor was absorbed increasingly with the increase of the concentrations of AMCs. The adsorbed response was achieved after 10 min of evaporation and the recovery response was found to change nonlinearly with changing concentration, and it was confirmed that a higher concentration of volatile simethicone led to a longer recovery time.

Significantly, the OMF sensor with a diameter of 2.5 $\mu$m exhibited a rapid response, as shown in Figure 6(a). The peak of additional loss can reach up to 0.0458 dB at a concentration of 25.7 mg/m$^3$ and 17.102 dB at 134.2 mg/m$^3$, respectively. However, as observed in Figures 6(b) and 6(c), for the other two OMF sensors with different diameters, the peak of additional loss was approximately 0.016 dB and 0.007 dB at the concentration of 25.7 mg/m$^3$ with diameters of 5 $\mu$m and 6 $\mu$m, respectively. This was because the additional loss increases with decreasing of the OMF diameter [17].

It was clear from Figure 6(d) that the sensitivities of the three coated OMF sensors with different diameters at the same concentration of 106.3 mg/m$^3$ were evidently different. The highest sensitivity of approximate 0.0263 dB/mg/m$^3$ was obtained for the coated OMF sensor with a diameter of 2.5 $\mu$m, and values of 0.0024 dB/mg/m$^3$ and 0.0018 dB/mg/m$^3$ were found with the other two OMF sensors with diameters of 5 $\mu$m and 6 $\mu$m, respectively. It exhibited more sensitive compared with reference [9], as showed in Table 1. Consequently, the diameter of the tested OMF sensor plays an important role in measuring the concentration of the AMCs.

*4.3. Reliability of Coated OMF.* In order to verify the repeatability of the OMF sensor's response, the AMC coating was cleaned using alcohol several times. Figure 7 showed the

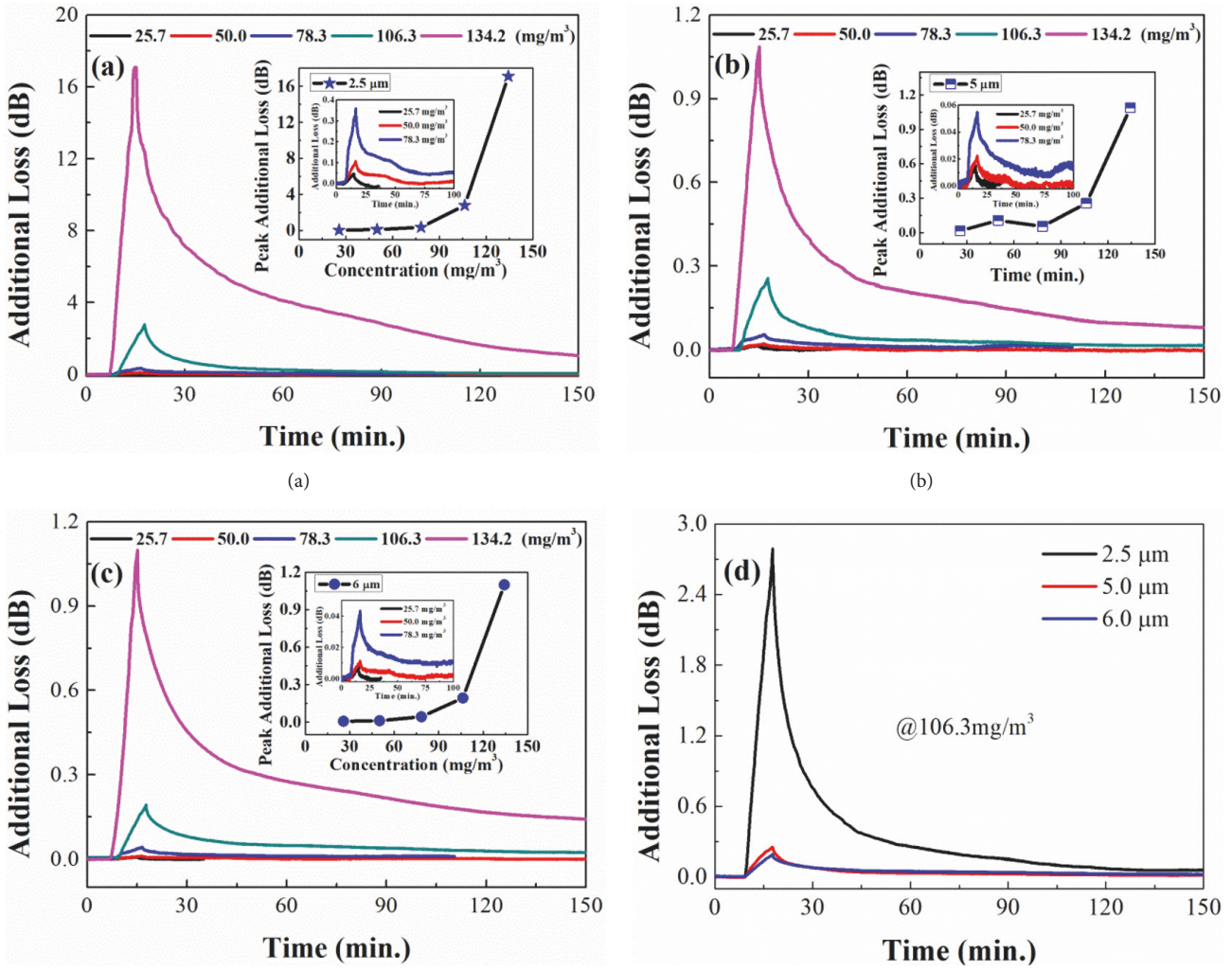


FIGURE 6: Responses of coated OMF sensor at different concentrations of AMCs from 25.7 to 134.2 mg/m$^3$ with three different diameters of (a) 2.5 $\mu$m, (b) 5 $\mu$m, and (c) 6 $\mu$m and (d) response results of OMF sensor obtained at 106.3 mg/m$^3$ with three different diameters.

TABLE 1: Summary of the responses shown by each sensor to the different concentrations.

| Content | This paper | | | Reference [9] |
|---|---|---|---|---|
| **Diameter ($\mu$m)** | 2.5 | 5 | 6 | 7 |
| **Concentration (mg/m$^3$)** | 106.3 | 106.3 | 106.3 | $1 \times 10^6$ |
| **Response (dB)** | 2.79 | 0.26 | 0.19 | 6.64 |

results obtained during several times of cleaning, where the time between each alcohol cleaning was around 20 min, which suggested a consistent response of the OMF sensor, and the relative error of the initial response was about 10% to 12%. The proposed HSN-coated OMF sensors show good reliability, which will provide a new approach in monitoring volatile simethicone concentrations. In addition, the results also indicated that the coated OMF has a potential use to monitor AMCs online.

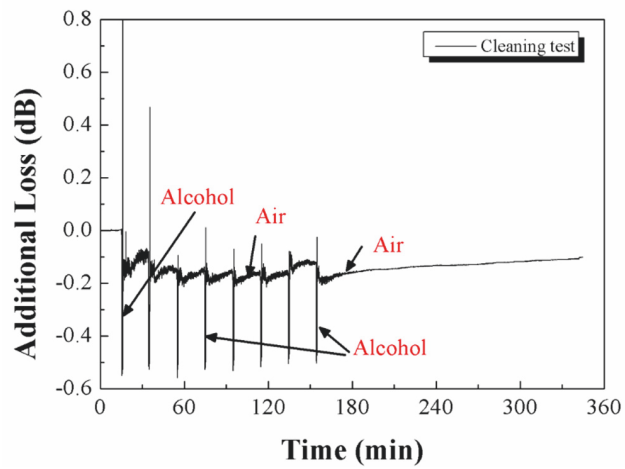


FIGURE 7: Repeatability of the response of an OMF sensor with a diameter of 5 $\mu$m when immersed in alcohol eight times.

## 5. Conclusions

We fabricated and measured the properties of a high sensitivity coated OMF sensor for AMCs. The tapered OMFs with diameters of 2.5 $\mu$m, 5 $\mu$m, and 6 $\mu$m were fabricated by using a high-precision electrically controlled setup. The coating of the OMF was produced by means of meniscus coating method. The relationship between the transmittance loss of the coated OMF and the AMC concentrations was obtained. The experimental results showed that the proposed coated OMF sensors exhibit high resolution and excellent sensitivity. For the volatile simethicone, the sensitivity of the OMF sensor was 0.0263 dB/mg/m$^3$ with a diameter of 2.5 $\mu$m and 0.0024 dB/mg/m$^3$ and 0.0018 dB/mg/m$^3$ for the OMFs with diameters of 5 $\mu$m and 6 $\mu$m, respectively. In addition, the repeatable responses of the coated OMF sensor system showed that the coated OMF sensor could be used in the online monitoring of AMCs. Furthermore, the sensor system exhibited high sensitivity and repeatability.

## Data Availability

The data used to support the findings of this study are available from the corresponding author upon request.

## Conflicts of Interest

The authors declare that there are no conflicts of interest regarding the publication of this paper.

## Authors' Contributions

Longfei Niu and Guorui Zhou contributed equally to this work.

## Acknowledgments

This work was supported by the National Natural Science Foundation of China (Grants nos. 51535003, 61605186, and 61705205).

## References

[1] V. K. Rai, "Temperature sensors and optical sensors," *Applied Physics B: Lasers and Optics*, vol. 88, no. 2, pp. 297–303, 2007.

[2] W. Li, Z. Hu, X. Li et al., "High-sensitivity microfiber strain and force sensors," *Optics Communications*, vol. 314, pp. 28–30, 2014.

[3] S. Poeggel, D. Tosi, D. Duraibabu, G. Leen, D. McGrath, and E. Lewis, "Optical fibre pressure sensors in medical applications," *Sensors*, vol. 15, no. 7, pp. 17115–17148, 2015.

[4] H. García-Miquel, D. Barrera, R. Amat, G. V. Kurlyandskaya, and S. Sales, "Magnetic actuator based on giant magnetostrictive material Terfenol-D with strain and temperature monitoring using FBG optical sensor," *Measurement*, vol. 80, pp. 201–206, 2016.

[5] C. Elosua, I. R. Matias, C. Bariain, and F. J. Arregui, "Airborne molecular compound optical fiber sensors: A review," *Sensors*, vol. 6, no. 11, pp. 1440–1465, 2006.

[6] L. Tong, R. R. Gattass, J. B. Ashcom et al., "Subwavelength-diameter silica wires for low-loss optical wave guiding," *Nature*, vol. 426, no. 1825, pp. 816–819, 2003.

[7] L. Tong, J. Lou, and E. Mazur, "Single-mode guiding properties of subwavelength-diameter silica and silicon wire waveguides," *Optics Express*, vol. 12, no. 6, pp. 1025–1035, 2004.

[8] S. K. Khijwania and B. D. Gupta, "Fiber optic evanescent field absorption sensor with high sensitivity and linear dynamic range," *Optics Communications*, vol. 152, no. 4-6, pp. 259–262, 1998.

[9] J. Luo, J. Yao, and W. Wang, "Melamine sensing based on evanescent field enhanced optical fiber sensor," in *International Symposium on Photoelectronic Detection and Imaging 2013: Fiber Optic Sensors and Optical Coherence Tomography*, 2013.

[10] J. C. Echeverria, P. de Vicente, J. Estella, and J. J. Garrido, "A fiber-optic sensor to detect airborne molecular compounds based on a porous silica xerogel film," *Talanta*, vol. 99, pp. 433–440, 2012.

[11] C.-S. Park, Y. Han, K.-I. Joo, Y. W. Lee, S.-W. Kang, and H.-R. Kim, "Optical detection of airborne molecular compounds using selective tensile effects of a polymer-coated fiber Bragg grating," *Optics Express*, vol. 18, no. 24, pp. 24753–24761, 2010.

[12] D. Liu, W. Han, A. K. Mallik et al., "High sensitivity sol-gel silica coated optical fiber sensor for detection of ammonia in water," *Optics Express*, vol. 24, no. 21, pp. 24179–24187, 2016.

[13] A. Farooq, R. Al-Jowder, R. Narayanaswamy, M. Azzawi, P. J. R. Roche, and D. E. Whitehead, "Gas detection using quenching fluorescence of dye-immobilised silica nanoparticles," *Sensors and Actuators B: Chemical*, vol. 183, no. 20, pp. 230–238, 2013.

[14] C.-T. Wang, C.-L. Wu, I.-C. Chen, and Y.-H. Huang, "Humidity sensors based on silica nanoparticle aerogel thin films," *Sensors and Actuators B: Chemical*, vol. 107, no. 1, pp. 402–410, 2005.

[15] X. Zou, C. Tao, L. Yan et al., "One-step sol-gel preparation of ultralow-refractive-index porous coatings with mulberry-like hollow silica nanostructures," *Surface & Coatings Technology*, 2018.

[16] C. Tao, H. Yan, X. Yuan et al., "Synthesis of shape-controlled hollow silica nanostructures with a simple soft-templating method and their application as superhydrophobic antireflective coatings with ultralow refractive indices," *Colloids and Surfaces A: Physicochemical and Engineering Aspects*, vol. 501, pp. 17–23, 2016.

[17] G. Zhou, X. Yuan, H. Lü et al., "A contamination sensor based on an array of microfibers with nanoscale-structured film," *Advances in Condensed Matter Physics*, vol. 2014, pp. 1–6, 2014.

[18] W. Stöber, A. Fink, and E. Bohn, "Controlled growth of monodisperse silica spheres in the micron size range," *Journal of Colloid and Interface Science*, vol. 26, no. 1, pp. 62–69, 1968.

[19] C. Tao, H. Yan, X. Yuan et al., "Sol-gel based antireflective coatings with superhydrophobicity and exceptionally low refractive indices built from trimethylsilanized hollow silica nanoparticles," *Colloids and Surfaces A: Physicochemical and Engineering Aspects*, vol. 509, pp. 307–313, 2016.

[20] C. Tao, H. Yan, X. Yuan et al., "Sol–gel preparation of moisture-resistant antireflective coatings from novel hollow silica nanoparticles," *Journal of Sol-Gel Science and Technology*, vol. 80, no. 2, pp. 538–547, 2016.